Conceptual Modeling of Jet Propulsion

Bachelor's Thesis
by

Himani Sinhmar (140010061)

under the guidance of

Prof. S.P. Mahulikar

Department of Aerospace Engineering
Indian Institute of Technology, Bombay
Mumbai 400 076

Contents

List of Figures

Chapter 1

Introduction

The approach to the analysis of the mechanics of jet propulsion is largely based on the changes to the parameters of the fluid which interacts with the engine. In stage one of BTP, I have explored the first principles of jet propulsion by estimating the pressure forces acting on a simplified model of turbojet engine (Toy model). In a jet engine thrust is generated by pressure forces exerted by the fluid on its boundaries and components. Theoretically thrust and propulsive efficiency are sufficient for the understanding of the evolution of variety of aircraft engines. The model developed exhibited that an engine which can make maximum possible use of fluid pressure profile for thrust would have the highest possible propulsive efficiency. The toy model considered, consists of diverging diffuser and converging nozzle both connected by combustion chamber that was modeled as a surface with step change in thermodynamic parameters, as shown in Fig.1.1

In the stage two of BTP I have further carried out the work by analyzing the physical model of turbojet engine. The modeling of theoretical turbojet engine would differ based on the type of heat addition taking place in the combustor (assuming isentropic compression and expansion in the inlet-compressor and the turbine-nozzle region). Heat addition can take place either via constant pressure combustion in a variable area duct or via variable pressure combustion in constant area duct. Both the models are discussed here. This model is then extended to ramjet engines such that efficient use of pressure profile is made to achieve higher values of net thrust. The results indicate that net thrust and propulsive efficiency depend on the engine geometry, inlet velocity and combustion temperature. Inlet-diffuser of ramjet is modeled as converging diverging region. Combustion chamber is modeled as constant area duct i.e. variable pressure combustion takes place. Nozzle is also modeled as converging-diverging region. Detailed performance analysis of ideal

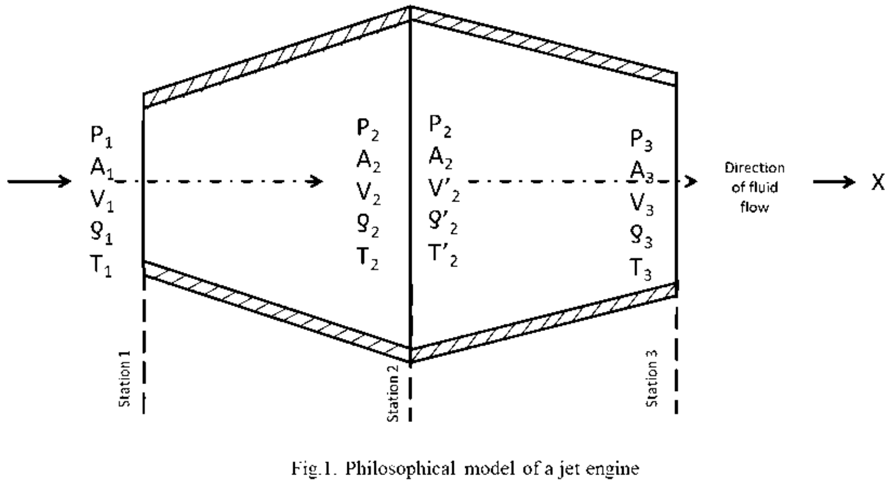

Figure 1.1: Toy model of turbojet engine

ramjet with flight conditions, operational conditions and geometrical parameters is carried out.

Chapter 2

Theoretical Model 1 of Turbojet Engine

This model consider variable pressure combustion that is heat addition taking place in constant area duct.Fig.2.1 shows the theoretical model of jet engine. Station 1 is the inlet and 3 is the exit. Station 2 to 2' is the combustion chamber such that area A_2 is equal to $A_{2'}$.

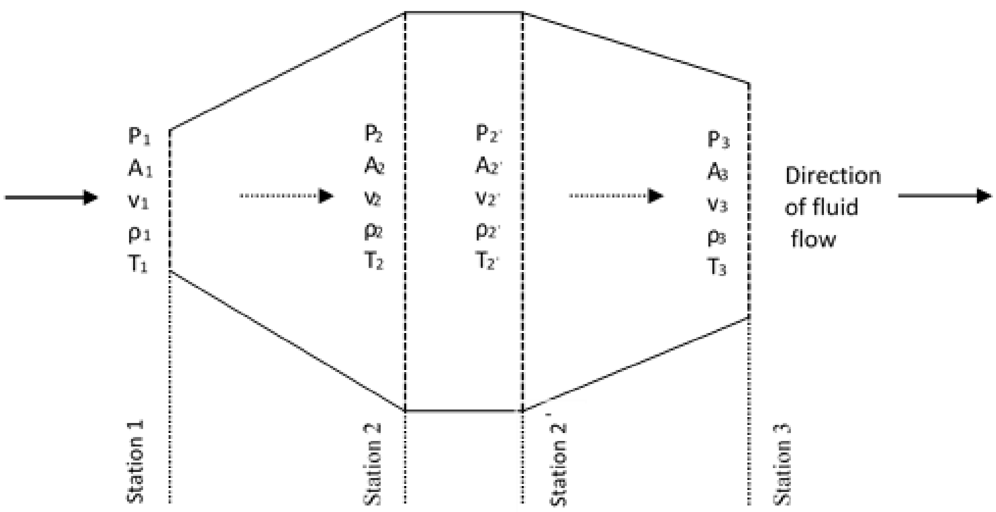

Figure 2.1: Theoretical model of turbojet engine for variable pressure combustion

Due to heat addition there is an increase in the temperature from T_2 to $T_{2'}$ and a decrease in the pressure from P_2 to $P_{2'}$ which results in reduction of density from ρ_2 to $\rho_{2'}$. This can be explained based on the Rayleigh curve (1), as the flow is subsonic at the entrance of the combustion chamber, heat addition leads to an increase in Mach number, decrease in pressure and an increase in velocity. For optimal expansion, the pressure at station 3 is P_1 (same as that at station 1). All the dynamic head is provided by the compressor in a practical jet engine and the ram flow is provided by means of the velocity v_1 at station 1. This does not include the dynamic head needed to run the compressor. The flow passage from station 1 to 2 corresponds to the subsonic diffusion in the intake and the compressor. In a practical compressor, in addition to the stator, diffusion also occurs in the rotor and the amount of diffusion in the rotor is indicated by the degree of reaction of the stage. Hence the region from station 1 to 2 represents the intake and the compressor in a practical jet engine and the region from station 2' to 3 represents the turbine and the nozzle. As shown in Fig.1, from station 1 to 2 the flow track area keeps increasing. A similar argument can be put forth to explain the decreasing flow track area from station 2' to 3.

2.1 Thrust provided by jet engine

A high pressure ratio is desirable as thermodynamics claims that the basic cycle efficiency increases with pressure ratio and higher operating temperature enables higher amount of work to be obtained from the basic thermodynamics cycle. This is also reflected in the mathematical definition for thrust

$$F = \int_1^2 (P - P_\infty) cos\beta \ \mathrm{d}s \quad + \quad \int_{2'}^3 (P - P_\infty) cos\beta \ \mathrm{d}s \tag{2.1}$$

$$F = \int (P - P_\infty) cos\beta \ \mathrm{d}s \tag{2.2}$$

where the integral has to be performed over the entire surface of the jet engine and its components.

2.2 Approach developed to compute thrust

In the case of optimal expansion, the pressure increases from P_1 to P_2 in the diffuser region from station 1 to 2 and drops back to P_1 at station 3. If the temperature is not raised at station 2 then A_3 would be equal to A_1 and no thrust would be obtained as is indicated by Eq. (2.1). β is the angle subtended by the outward normal with the direction of motion of the aircraft. From station 1 to 2, $cos\beta$ takes a constant negative value. For an isentropic flow how the area varies from station 1 to 2 or station 2' to 3 does not change the final parameters. Here, flow from station 1 to 2 and station 2' to 3 is assumed to be isentropic. Therefore, final thermodynamic parameters do not depend on nature of the radius variation but only on the local value of the radius. From station 1 to 2 and station 2' to 3 remains constant. Hence Eq. (2.2) may be written as

$$F = cos\beta_{1-2} \int_{1}^{2} (P - P_{\infty}) \, \mathrm{d}s \quad + \quad cos\beta_{2'-3} \int_{2'}^{3} (P - P_{\infty}) \, \mathrm{d}s \tag{2.3}$$

To account for the $cos\beta$ ds term in Eq. (2.2), the pressure may be projected on two annular disks as shown in Fig.2.2. The two disks 1 to 2 and 2' to 3 have outer radii r2. The inner radius of disk 1 to 2 is r1 while that of disc 2' to 3 is r_3 , where r_1 ¡ r_3. Heating the flow at station 2 reduces the density of fluid in the region 2' to 3 and to maintain continuity the flow track area increases, thereby reducing the area projected of disc 2' to 3 in Fig.2.2. It is because of this reduction in area of disc 2' to 3 due to the rise in temperature that generates thrust.

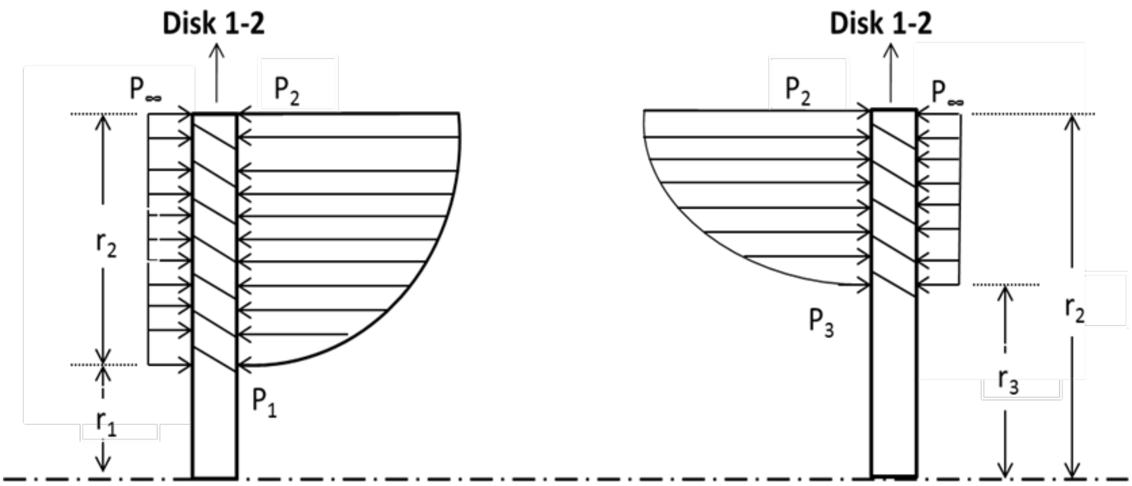

Fig.3. Projection of pressure profile

Figure 2.2: Projection of pressure profile

The evaluation of thrust of the jet engine shown in Fig.1. now reduces to the evaluation of forces acting on the discs 1 to 2 and 2' to 3 and subtracting them.

Hence Eq (2.2) now reduces to Eq.(2.4) and Eq.(2.5) where P(r) is found by solving the governing equation of fluid flow.

$$F = \int_{\mathrm{Disk}_{1-2}} (P(r) - P_\infty)\ \mathrm{d}A \quad \int_{\mathrm{Disk}_{2'-3}} (P(r) - P_\infty)\ \mathrm{d}A \tag{2.4}$$

$$F = \int_{r_1}^{r_2} (P(r) - P_\infty) 2\pi r\ \mathrm{d}r \quad \int_{r_{2'}}^{r_3} (P(r) - P_\infty) 2\pi r\ \mathrm{d}r \tag{2.5}$$

2.3 Redefining Propulsive Efficiency

In a jet engine if thrust is to increase in addition to increase in $P_{2'}$, $T_{2'}$ must increase in order to reduce the negative thrust. In a jet engine negative thrust is always present because $T_{2'}$ cannot increase indefinitely due to limitations in material cooling technology. Due to the presence of negative thrust, fluid forces cannot be utilized fully for the generation of net thrust. A propulsive efficiency is defined in order to indicate how efficiently the fluid pressure forces are used for the generation of thrust. It may be mathematically defined as

$$\eta_p = \frac{\int (P - P_\infty) cos\beta\ \mathrm{d}s}{\int (P - P_\infty)\ \mathrm{d}s} \tag{2.6}$$

2.4 Numerical Modeling of Theory Proposed

It is assumed that the flow is steady, inviscid and quasi 1 dimensional. Further, the gas is assumed to be calorically perfect and the contribution of the fuel mass flow rate to the gas in the duct is small. Hence, combustion is modeled as heat transfer through the wall. The pressure forces acting on the engine can be derived from first principles using conservation laws and isentropic flow equations. Following analysis is carried out for subsonic inlet flow with optimal expansion in the nozzle that is, P_3 is equal to P_1. P_1 and T_1 depend on the altitude at which the aircraft is flying and hence are known. Also, M_∞ is different from M_1 as explained above. Thermodynamic parameters at station 2 are solved using conservation equations and equation of state.

$$\frac{v_1 A_1}{A_2} = \left(\frac{P_2}{P_1}\right)^{\frac{1}{\gamma}} \sqrt{2c_p\left(T_{01} - T_1\left(\frac{P_2}{P_1}\right)^{\frac{\gamma-1}{\gamma}}\right)} \tag{2.7}$$

$$where \quad T_{01} = T_1(1 + \frac{\gamma - 1}{2}M^2) \tag{2.8a}$$

$$v_2 = \sqrt{2c_p\left(T_{01} - T_1\left(\frac{P_2}{P_1}\right)^{\frac{\gamma-1}{\gamma}}\right)} \tag{2.8b}$$

$$T_2 = T_1\left(\frac{P_2}{P_1}\right)^{\frac{\gamma-1}{\gamma}} \tag{2.8c}$$

Similarly, the pressure variation in region 1 to 2 is obtained using Eq.(2.8) and Eq. (2.7). From station 1 to 2 and station 2' to 3 engine is modeled with a constant β. For station 2 to 2'

$$\frac{P_{2'}}{P_2} = \frac{1 + \gamma M_2^2}{1 + \gamma M_{2'}^2} \tag{2.9}$$

$$M_{2'} = M_2\frac{P_2}{P_{2'}}\sqrt{\frac{T_{2'}}{T_2}} \tag{2.10}$$

$T_{2'}$ is the turbine inlet temperature that is limited by the maximum temperature that turbine blades can sustain. Using Eq. (2.9) and Eq. (2.10), P_2 and M_2 are calculated. It is assumed that the Cp (specific heat at constant pressure) of the fuel-air mixture is approximately the same as the Cp of ambient air. For a given M_1, combustion temperature $T_{2'}$ will vary with $\frac{A_2}{A_1}$ .i.e. the size of the jet engine. This is to satisfy the condition that turbine inlet Mach number ($M_{2'}$) is always subsonic and the exit Mach number $M_3 \leq 1$. Eq (2.11) and Eq (2.12) are used to obtain the range of the $T_{2'}$ for a given $\frac{A_2}{A_1}$.

$$M_{2'} = \frac{T_{2'}v_2}{T_2\sqrt{\gamma R T_{2'}}} \quad < 1 \tag{2.11}$$

$$M_3 = \sqrt{\frac{2}{\gamma - 1}\left(T_{2'}\left(\frac{1 + \frac{\gamma-1}{2}\left(\frac{T_{2'}v_2}{T_2\sqrt{\gamma R T_{2'}}}\right)^2}{T_{2'}\left(\frac{P_1}{P_2}\right)}\right) - 1\right)} \tag{2.12}$$

As the exit pressure P_3 is known ($=P_1$), exit Mach number M_3 is calculated using Eq.(2.13)

$$M = \sqrt{\left(\left(\frac{P_{02'}}{P}\right)^{\frac{\gamma-1}{\gamma}} - 1\right)\left(\frac{2}{\gamma-1}\right)} \tag{2.13}$$

$$P_0 = P\left(1 + \frac{\gamma-1}{2}M_2^2\right)^{\frac{\gamma}{\gamma-1}} \tag{2.14}$$

$$T_0 = T\left(1 + \frac{\gamma-1}{2}M_2^2\right) \tag{2.15}$$

The sonic conditions are denoted by an asterisk. It can be shown that for an isentropic flow in a variable area duct

$$\left(\frac{A}{A^*}\right)^2 = \frac{1}{M^2}\left[\frac{2}{\gamma-1}\left(1 + \frac{\gamma-1}{2}M^2\right)\right]^{\frac{\gamma+1}{\gamma-1}} \tag{2.16}$$

It can also be shown that for an isentropic flow A* is constant1. Using Eq. (2.16) at station 2', A* is obtained for region 2' to 3. Similarly, A_3 is obtained from Eq. (2.16) using M_3. Mach number and the pressure acting at all points is obtained from Eq. (2.16) and Eq. (2.13) respectively in region 2' to 3. Net thrust provided by the engine is given by Eq. (26). Table 1 shows the sample calculation for obtaining net thrust by following the above approach.

2.5 Mathematical proof for the claim: Exit area > Inlet area for net thrust to be positive

For subsonic flow, relation between $\frac{A}{A^*}$ vs M is given by Eq. 2.17. and is shown in Fig.2.4. As can be seen $\frac{A}{A^*} \propto \frac{1}{M}$. Critical Area, A^*, always increases on addition of heat in a duct with subsonic inlet mach number as proved below. Applying continuity Eq.(2.18) on the two critical sections (before addition of heat and after addition of heat).

$$\rho_1^* A_1^* a_1^* = \rho_2^* A_2^* a_2^*$$

$$Using \quad equation \quad of \quad state \quad \frac{\rho_1^*}{\rho_2^*} = \frac{P_1^* T_2^*}{P_2^* T_1^*}$$

$$which \quad gives \quad \frac{A_2^*}{A_1^*} = \frac{P_1^*}{P_2^*}\sqrt{\frac{T_2^*}{T_1^*}}$$

$\frac{A_2}{A_1}$	3	$\frac{A_{2'}}{A_3}$	1.36
P_1	101325 Pa	P_{01}	1.608334×10^5 Pa
T_1	288.15 K	P_{02}	1.475274×10^5 Pa
M_1	.84	$\frac{A_3}{A_1}$	2.21
P_2	1.567232×10^5 Pa	F_{1-2}	38108.64 N
T_2	326.39 K	$F_{2'-3}$	5751.34 N
M_2	.19	F_{net}	32357.3 N
$M_{2'}$	.45	$\dot{m}$	147.39 kg
$P_{2'}$	1.282863×10^5 Pa	$F_{\text{conventional}}$	32354.83 N
$T_{2'}$	1200 K	$\eta_{\text{redefined}}$	15.34%
M_3	.75	$\eta_{\text{conventional}}$	57.55%

Table 2.1: Sample calculations for variable pressure combustion

From isentropic relations, $\frac{P_1^*}{P_2^*} = \frac{P_{01}}{P_{02}}$.

$$\frac{A_2^*}{A_1^*} = \frac{P_{01}}{P_{02}}\sqrt{\frac{T_2^*}{T_1^*}}$$

Because of heat addition temperature increases, giving $T_2^* > T_1^*$. For entropy to be positive, total pressure decreases after heat addition for subsonic flow implying $P_{01} > P_{02}$.Therefore from above equation,

$$A_2^* > A_1^*$$

From isentropic relation (Eq. 2.13) we can see that Mach number is directly proportional to corresponding total pressure P_0. So we can write $\frac{A}{A^*} \propto \frac{1}{P_0}$ as shown in Fig.2.3 Applying the above relation to station 1 and station 3

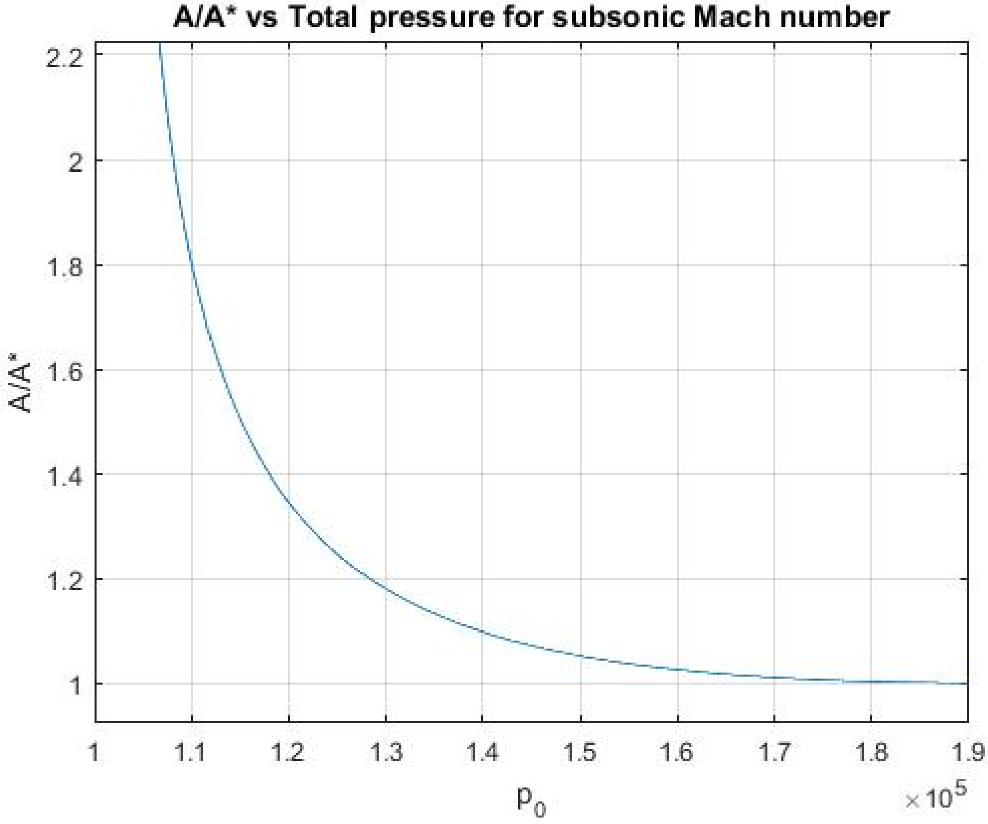

Figure 2.3: Variation of $\frac{A}{A^*}$ with P_0 for subsonic Mach number

$$\frac{A_1}{A_1^*} \propto \frac{1}{P_{01}}$$
$$\frac{A_3}{A_2^*} \propto \frac{1}{P_{02}}$$
$$As \quad P_{01} > P_{02} \implies \frac{A_1/A_1^*}{A_3/A_2^*} = \frac{P_{02}}{P_{01}}$$
$$i.e. \quad \frac{A_1}{A_1^*} < \frac{A_3}{A_2^*} \implies A_3 > A_1$$

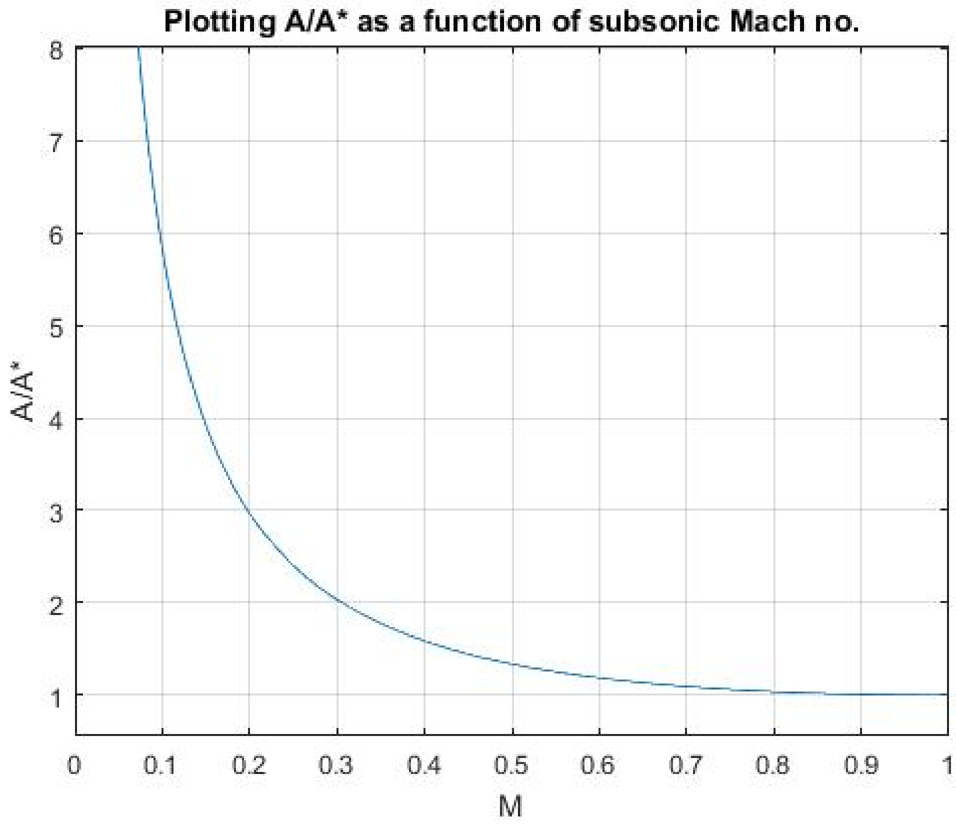

Figure 2.4: Variation of $\frac{A}{A^*}$ with subsonic Mach number

2.6 Comparing thrust and efficiency with those obtained using conventional method

The exact formula for efficiency of air-breathing engines as given in the literature is (2)

$$\eta_p = \frac{2}{1 + \frac{c}{v}} \tag{2.17}$$

where c is the exhaust speed, and v is the speed of the aircraft. It lies in the range 0.2 - 0.9. In this case substituting the values of c ($= M_3$ a_3) and v ($= M_\infty$ a_∞), η_p comes out to be 57.55%. The expression for thrust using Newtons laws is given by

$$\dot{m} = \rho_1 A_1 v_1 \tag{2.18}$$

$$\text{Thrust}_{\text{conventional}} = \dot{m}(v_4 - v_1) \tag{2.19}$$

As shown in table 1, the thrust values obtained by integrating the pressure forces and as given by Newtons laws ($F_{\text{conventional}}$) are equal, as expected. But the propulsive efficiency differs by a large margin which suggests that only a small fraction of the pressure forces are utilized to generate net thrust, and hence the engine model can be further improved for better utilization of pressure forces. This is because conventional efficiency ($\eta_{p_{\text{conventional}}}$) indicates the fraction of the net mechanical output that is converted into thrust power, whereas redefined propulsive efficiency ($\eta_{p_{\text{redefined}}}$) is an indicator of how efficiently an engine makes use of pressure profile. In an turbojet engine large fraction of thrust is negative thrust due to comparable exit area and inlet area, hence lower $\eta_{p_{\text{redefined}}}$. The thrust power generated is much higher than the kinetic energy intake and so $\eta_{p_{\text{conventional}}}$ has a higher value.

2.7 Discussion of results obtained

Numerical modeling is done in Maple for the above discussed model.

The variation of static pressure in region 1-2 is plotted in Fig2.5. This happens due to increase in flow track area of the subsonic flow and hence decrease in velocity (to maintain continuity) while there is an expansion occurring in region 2'-3 due to decrease in flow track area(Fig.2.7). This is also expected as diffusion takes place in the inlet and compressor of an airbreathing engine and expansion occurs in the turbine and nozzle .

Due to heat addition in the combustion chamber total pressure will differ in two regions. It can be shown that addition of heat in constant area duct leads to increase in the entropy of the flow implying that total pressure decreases after heat addition i.e. $P_{01} > P_{02}$.

The results obtained after numerical modeling indicate that thrust depends on the following parameters: inlet velocity (v_1), combustion temperature ($T_{2'}$) and area ratio ($\frac{A_2}{A_1}$). Once the dimensions of the engine are fixed (i.e. $\frac{A_2}{A_1}$ is fixed) thrust increases with the combustion temperature ($T_{2'}$) and inlet velocity v_1 as can been seen in the Fig.2.7.

The redefined propulsive efficiency increases with increase in turbine inlet temperature while it is approximately constant with the variation of the inlet velocity

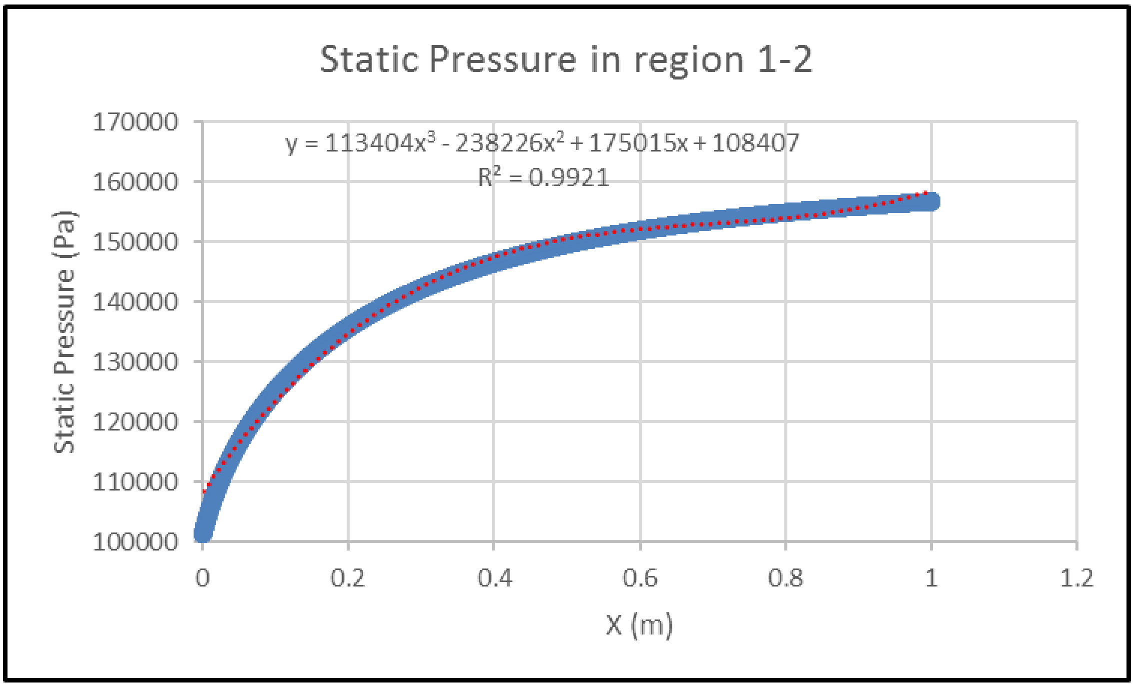

Figure 2.5: Variation of static pressure in region 1-2 (Variable pressure combustion)

as shown in Fig.2.8 This can be explained as on increasing the operating temperature the work output from the engine increases, increasing the net thrust.

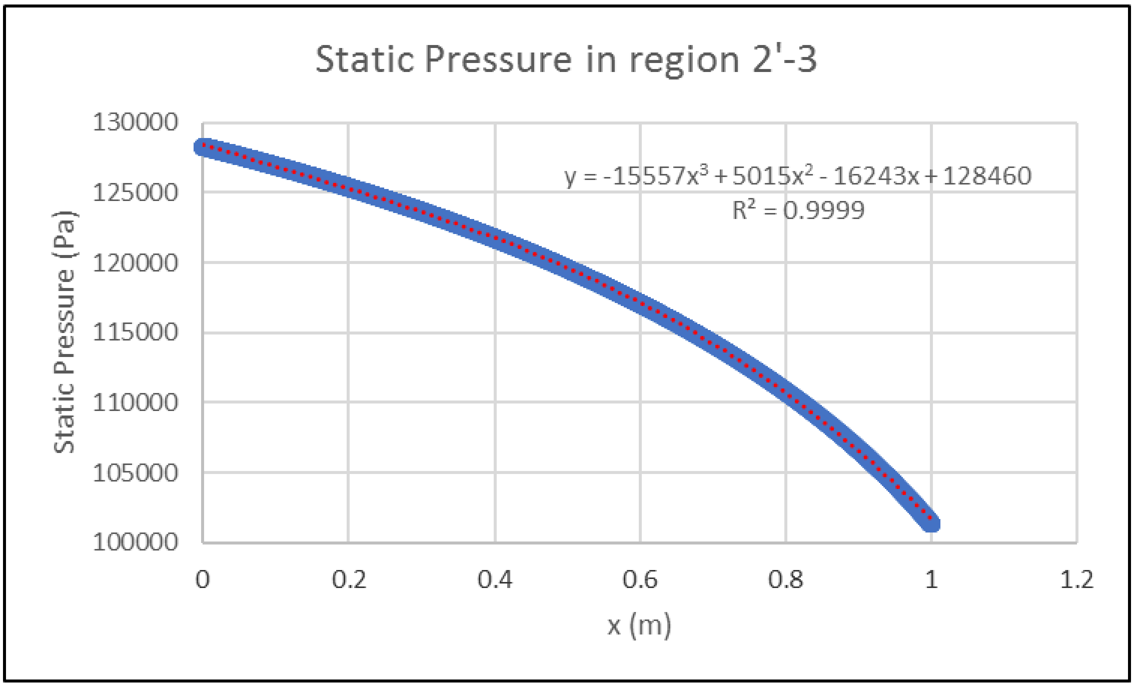

Figure 2.6: Variation of static pressure in region 2'-3 (Variable pressure combustion)

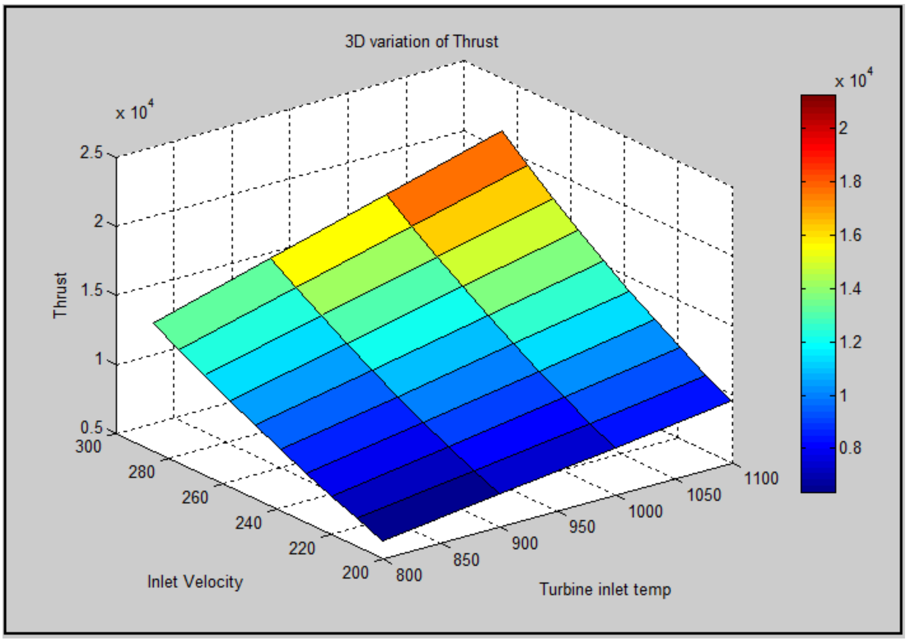

Figure 2.7: 3-D plot exhibiting the variation of net thrust with inlet velocity and combustion temperature (Variable pressure combustion)

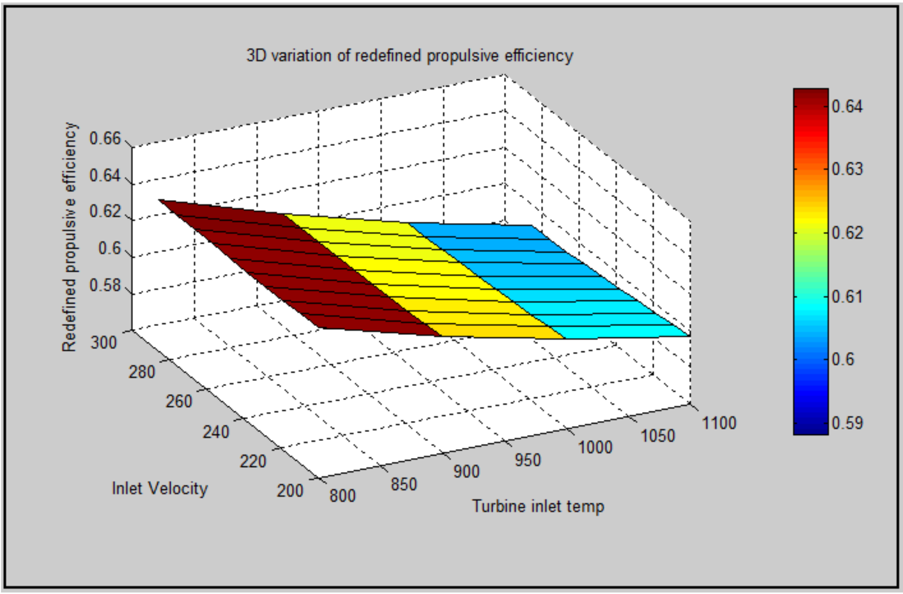

Figure 2.8: 3 D plot exhibiting the variation of redefined propulsive efficiency with inlet velocity and turbine inlet temperature (Variable pressure combustion)

Chapter 3

Theoretical Model 2 of Turbojet Engine

In this chapter second model for turbojet engine is tackled.

3.1 Constant pressure combustion in variable area duct

From the viewpoint of thermodynamic cycle efficiency, constant pressure combustion differs from variable pressure combustion and thus it is considered here. A variable area combustor that maintains a constant pressure is analyzed. Numerical modeling remains the same except that the flow parameters at 2' will be different now. Conservation laws are applied to the slab of the fluid as shown in Fig.3.1.

The continuity equation gives

$$\rho A v = (\rho + d\rho)(A + dA)(v + dv) \implies \frac{dv}{v} + \frac{dA}{A} + \frac{d\rho}{\rho} \tag{3.1}$$

The balance of the momentum in the direction of motion gives

$$\dot{m}(v + dv) - \dot{m}v = pA - p(A + dA) + pdA \implies dv = 0 \tag{3.2}$$

Eq.(3.2) signifies a constant velocity flow i.e. $v_{2'} = v_2$. Then from continuity equation (2.18)

$$A_{2'}\rho_{2'} = A_2\rho_2 \implies A_{2'} = \frac{\rho_2 A_2 T_{2'} R}{P_2} \tag{3.3}$$

Since the combustor is modeled as a variable area duct, the outward normal of its surface subtends a positive angle (in I^{st} and IV^{th} quadrant) with the direction

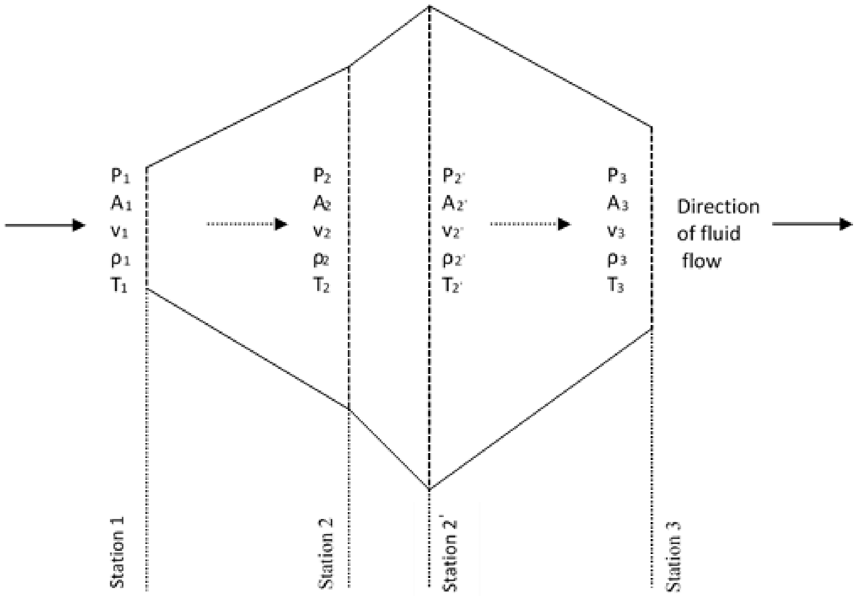

Figure 3.1: Theoretical model of turbojet engine for isobaric combustion

of the motion. Hence the pressure forces acting on it contribute towards positive thrust. Table 3.1 shows the calculations carried out using the same initial conditions as for constant area combustor modeling.

3.2 Comparing the Two models proposed

The conventional thermal efficiency is defined as the ability of an engine to convert the thermal energy inherent in the fuel (which is unleashed in a chemical reaction) to a net kinetic energy gain of the working medium.

$$\eta_{thermal} = \frac{\dot{m}_a\left[(1+f)\frac{u_e^2}{2} - \frac{u^2}{2}\right]}{\dot{m}_f Q_R} \tag{3.4}$$

$$For f << 1 \qquad \eta_{thermal} = \frac{\frac{u_e^2}{2} - \frac{u^2}{2}}{q} \tag{3.5}$$

Where ($\dot{m}_a$) is the mass flow rate of incoming air, (($\dot{m}_f$) is the mass flow rate of fuel injected, f is the ratio of the mass flow rate of air to the mass flow rate of fuel, Q_R is the heat of reaction of the fuel, q = fQ_R, u_e is the exhaust velocity and u is the inlet velocity. Basic thermodynamics claims that higher pressure ratio and

$\frac{A_2}{A_1}$	3
P_1	101325 Pa
T_1	288.15 K
M_1	.84
P_2	1.567232×10^5 Pa
T_2	326.39 K
M_2	.19
$M_{2'}$	.1004
$T_{2'}$	1200 K
M_3	.82
$\frac{A_{2'}}{A_2}$	3.67
$\frac{A_{2'}}{A_3}$	5.62

P_{01}	1.608334×10^5 Pa
P_{02}	1.578336×10^5 Pa
$\frac{A_3}{A_1}$	1.49
F_{1-2}	38108.64 N
$F_{2-2'}$	187245.956 N
$F_{2'-3}$	188469.022 N
F_{net}	36885.58 N
$\dot{m}$	147.39 kg
$F_{\text{conventional}}$	36878.77 N
$\eta_{\text{redefined}}$	5.12%
$\eta_{\text{conventional}}$	55.16%

Table 3.1: Sample calculations for constant pressure combustion

higher operating temperature increase the efficiency of the Brayton cycle. Table 3.2 shows a comparison between the two models. Isobaric combustion has a higher value of net thrust for similar conditions, because the normal to the surface of the isobaric combustor subtends an angle in first and fourth quadrant with the direction of motion of the aircraft and hence contributes towards net positive thrust.

The amount of heat addition required in variable pressure combustor is greater than that required for isobaric combustor. This is because of an increase in kinetic energy in variable pressure combustor which accounts for higher addition of heat for same combustor exit temperature. However, constant area combustor engines make better use of the pressure profile and have significantly higher redefined propulsive efficiency. Table 1 indicates a pressure decrease in constant area combustor ($P_{2'}$ $< P_2$) due to diffusion leading to an increase in exit area as compared to isobaric combustor (turbine inlet temperature is same for both cases), implying a lower

Parameters	Variable pressure combustion	Constant pressure combustion
F_{positive}	38108.64 N	225354.603 N
F_{negative}	5751.34 N	188469.022 N
F_{net}	32357.30 N	36885.58 N
$\eta_{p_{\text{redefined}}}$	15.34 %	5.12 %
$\eta_{p_{\text{conventional}}}$	57.55 %	55.16 %
η_{thermal}	9.02 %	11.22 %
$\eta_{\text{overall}_{\text{conventional}}}$	5.19 %	6.19 %
M_3	.75	.82
$\frac{A_3}{A_1}$	2.21	1.96
q	$9.626227\times10^5 J$	$9.159533\times10^5 J$

Table 3.2: Comparison between the two proposed models

value of negative thrust in the former. Due to the pressure drop in constant area combustor it does not require high negative gradient of flow track area in region 2' to 3 for optimal expansion and hence have higher exit area (A_3). This results in lower value of negative thrust and higher redefined propulsive efficiency.

3.3 Grid convergence

The grid generated for this numerical solution is one dimensional. The step size h is constant. Having chosen the number of elements, say N, pose h = $\frac{b-a}{N}$ where b is the last element and a, the first element. Now, define $x_i = x_0 +$ ih, with $x_0 =$ a and i = 0, 1, 2 N. In the model presented, the local pressure acting on the engine is just a function of radius and does not depend on the length of the engine. As the dependence of the pressure forces on the length of the engine would make it a perpetual motion machine generating thrust without heat addition and only by varying the length of the region 1 to 2 and 2' to 3. N is varied until the results obtained become independent of the length of the model. Then the solution is said to have converged for this value of N.

3.4 Mathematical Proof for the claim: Exit area > Inlet area for net thrust to be positive

Critical Area, A^*, always increases on addition of heat in a duct with subsonic inlet mach number as was proved in 2.5. In the isobaric turbojet engine, we have $P_{01} > P_{02} \implies \frac{A_1}{A_1^*} < \frac{A_3}{A_2^*}$ (Fig.2.3). As $A_2^* > A_1^*$, A_3 need to be greater than A_1 to satisfy this constraint.

3.5 Discussion of results

- The claim that the net positive thrust in a jet engine is generated due to an increase in exit area of engine (A3 > A1), proved in *2.5* and in *3.4*, is also validated by numerical modelling. Simulations carried out for different parameters (v_1, $T_{2'}$, $\frac{A_2}{A_1}$) results in $A_3 > A_1$ for net thrust to be positive. The exit area value plays an important role while comparing isobaric combustor and variable pressure combustor as discussed below.

- Isobaric combustion results in higher value of thrust due to contribution of positive thrust by the combustor. Heat addition is higher in variable pressure combustor due to increase in exit velocity of combustor with the same turbine inlet temperature and this increase in kinetic energy results in higher value of heat addition.

- The variable pressure combustor has a higher value of $\eta_{p_{\text{redefined}}}$ as compared to isobaric combustor this is because of the difference in the exit area of the two models. Variable pressure combustor has larger exit area due to drop in pressure in the combustor and so does not require high negative gradient of flow track area in region 2' to 3. This decreases the contribution of negative thrust in variable pressure combustor and thereby higher propulsive efficiency

- Redefined propulsive efficiency is much lower in magnitude as compared with conventional propulsive efficiency for both the cases. This is because conventional efficiency indicates the fraction of the net mechanical output that is converted into thrust power, whereas $\eta_{p_{\text{redefined}}}$ is an indicator of how efficiently an engine makes use of pressure profile. In a turbojet engine large fraction of thrust is negative thrust due to comparable exit area and inlet area, hence lower $\eta_{p_{\text{redefined}}}$. As the ratio of inlet and exit velocities is not too high $\eta_{p_{\text{conventional}}}$ has a higher value.

Chapter 4

Modeling Ideal Ramjet Engine

Ramjet engine is modeled with components : C-D diffuser, constant area duct combustor and C-D nozzle as shown in Fig.4.1. The assumptions for the flow

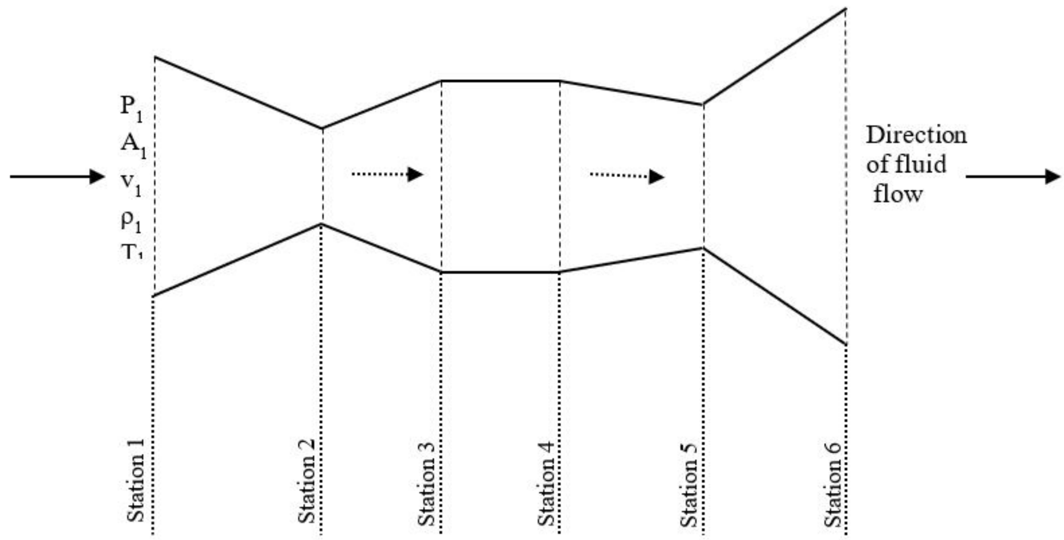

Figure 4.1: Model of ramjet engine (Variable pressure combustion)

are same as considered while modeling turbojet engine. No shock formation are considered. Optimal expansion is assumed with isentropic flow in C-D diffuser and C-D nozzle. The operational, geometrical and flight configuration of ramjet engine is shown in table 4.1. Upper limit of combustor exit temperature will be constrained by M_3 as would be discussed further.

M_1	3
Altitude	18 km
P_1	7504.84 Pa
T_1	216.65 K
A_1	Design variable
M_3	Design variable
P_6	P_∞

Table 4.1: Ramjet operational, geometrical and flight configuration

4.1 C-D Diffuser

Inlet area (A_1) is taken to be a design variable within 0.3 m^2 to 0.5 m^2. As inlet Mach number is supersonic, only one isentropic solution is possible where the throat area should be equal to critical area i.e. $A_2 = A^*$. Critical flow conditions (sonic flow) would be present at station 2. For subsonic combustion, the Mach number required at the exit of diffuser should be less than 0.3. So I have varied it as, $0.15 < M_3 < 0.3$. Given A_1 and M_1, A_2 is computed using Eq.(2.16). Thermodynamic parameters at station 2 and 3 are then calculated using isentropic equations, Eq.(2.13-2.15). As the flow is isentropic, total temperature and total pressure remains constant from station 1 to station 3. Diffuser compresses the flow to M < 0.3.

Static pressure variation in converging and diverging part of the diffuser is shown in Fig.4.2. Pressure increases in both the parts as expected.

4.2 Combustor : Constant area duct

The area remain constant in the combustor ($A_3 = A_4$) and so the pressure changes across combustor on addition of heat. For maximum work output combustion exit temperature should be maximum, as dictated by Brayton cycle. As no turbine blades are present at the exit of combustor, combustion exit temperature (T_4) can be as high as 3000 K. But the maximum value of T_4 is constrained by M_3 for

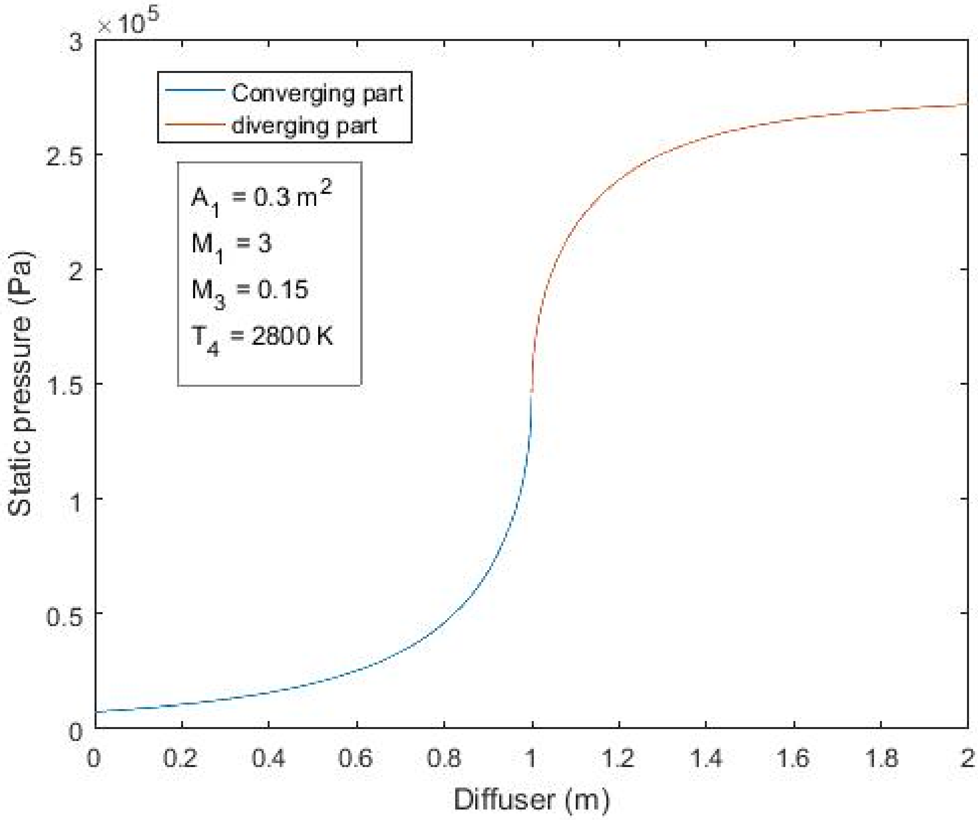

Figure 4.2: Variation of static pressure in C-D diffuser

solution of M_4 to be real from Eq.(4.1). Higher will be the combustion inlet Mach number the window for heat addition decreases to keep combustion exit number subsonic.

$$\frac{T_4}{T_3} = \left(\frac{1+\gamma M_3^2}{1+\gamma M_4^2}\right)^2 \left(\frac{M_4}{M_3}\right)^2 \tag{4.1}$$

$$\frac{P_4}{P_3} = \frac{1+\gamma M_3^2}{1+\gamma M_4^2} \tag{4.2}$$

Let $\beta = 1 + \gamma M_3^2$ and $\alpha = \frac{T_4}{T_3}$. Then from Eq.(4.1).

$$M_4^2 = \frac{\beta^2 - 2\alpha\beta + 2\alpha \pm \beta\sqrt{\beta^2 - 4\alpha\beta}}{2\gamma\alpha(\beta - 1)} \tag{4.3}$$

T_4 is taken to be 2800 K if substituting this gives a real solution to Eq.(4.3). If $\beta^2 - 4\alpha\beta$ is negative then solution to above equation does not exist and T_4 is given by Eq.(4.4). For $M_3 < .2029$, T_4 takes constant highest value, beyond this value of

M_3, T_4 decreases hyperbolically.

$$T_4 = T_3\left(\frac{\beta^2}{4(\beta-1)}\right) \tag{4.4}$$

Thermodynamic parameters at station 4 are then calculated from Eq.(4.2) and equation of state (P = ρRT). Variation of T_4 with M_3 is shown in Fig.4.3

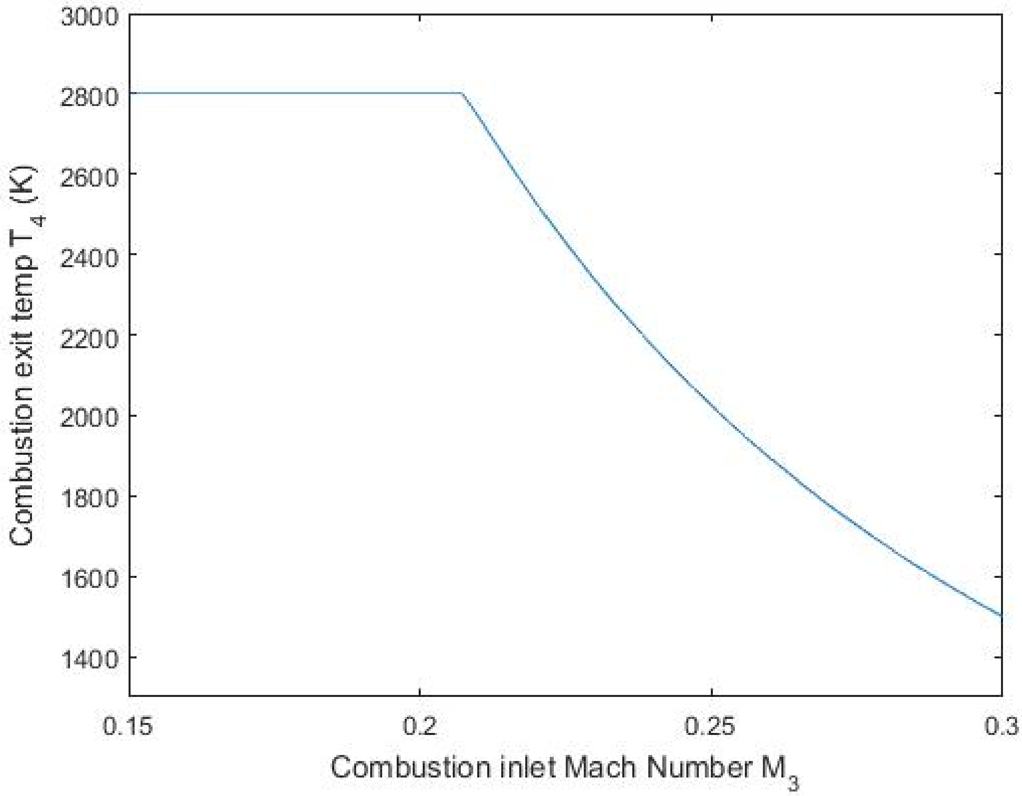

Figure 4.3: Variation of T_4 with M_3

4.3 C-D Nozzle

Nozzle accelerates the flow to supersonic Mach number from subsonic inlet Mach number. Again, only one isentropic flow solution will exist. Critical flow conditions exist at station 5, with $A_5 = A^*$. A_5 is calculated using Eq.(2.16), inlet flow condition to nozzle are known. Stagnation properties of the flow are changed due to heat addition in the combustor but will remain constant from station 4 to station

6. Optimal expansion condition is used to compute the thermodynamic parameters at station 6.

Static pressure variation in converging and diverging part of the nozzle is shown in Fig.4.4. Pressure decreases (expansion) in both the parts as expected.

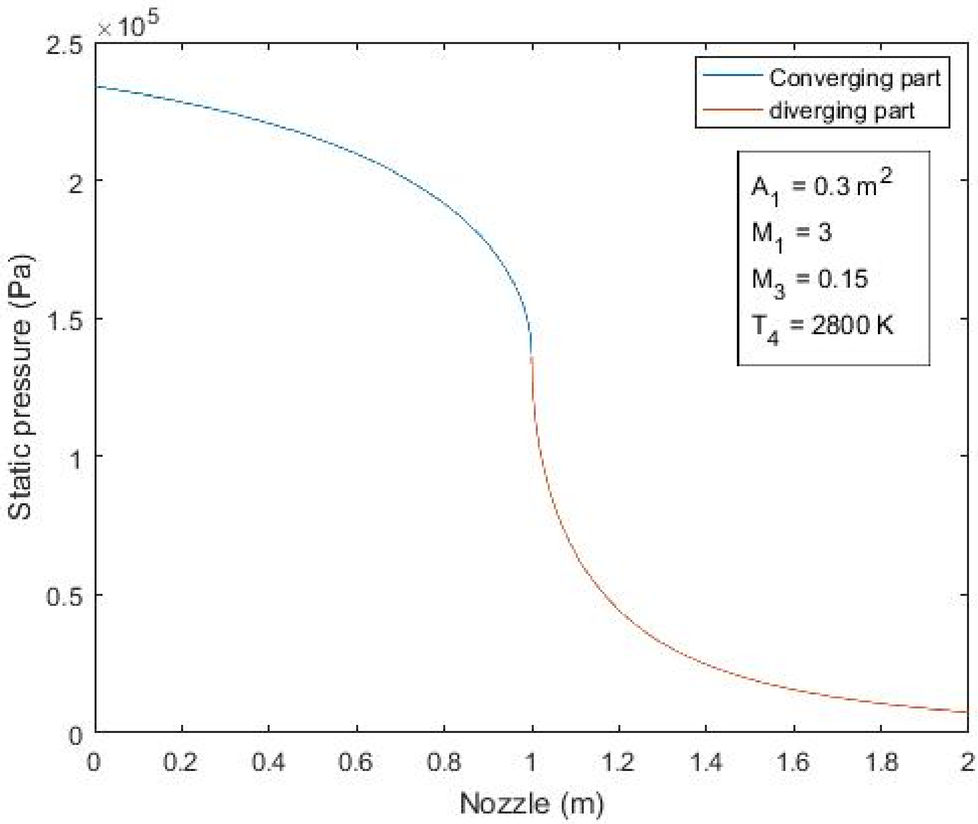

Figure 4.4: Variation of static pressure in C-D nozzle

4.4 Performance analysis

Thrust provided by diffuser and nozzle is computed using the procedure described in Chapter 2. Combustor does not contribute towards net thrust because it is modeled as a constant area duct.

Thrust variation with inlet area is plotted in Fig.4.5. Both the nozzle and diffuser % thrust remains constant with variation in A_1, because net thrust as well as nozzle/diffuser thrust vary linearly with inlet area as described by below equations.

$$\text{Thrust}_{\text{diffuser}} = A_1[\rho_1 v_1 v_3 - \rho_1 v_1^2 + \frac{f(M_3)}{f(M_1)}(P_3 - P_1)]$$

$$\text{where} \qquad f(M) = \frac{A}{A^*} \qquad \text{(fromEq.2.17)}$$

$$Thrust_{nozzle} = A_1[\rho_1 v_1 v_6 - \rho_1 v_1 v_4 + \frac{f(M_3)}{f(M_1)}(P_1 - P_4)]$$

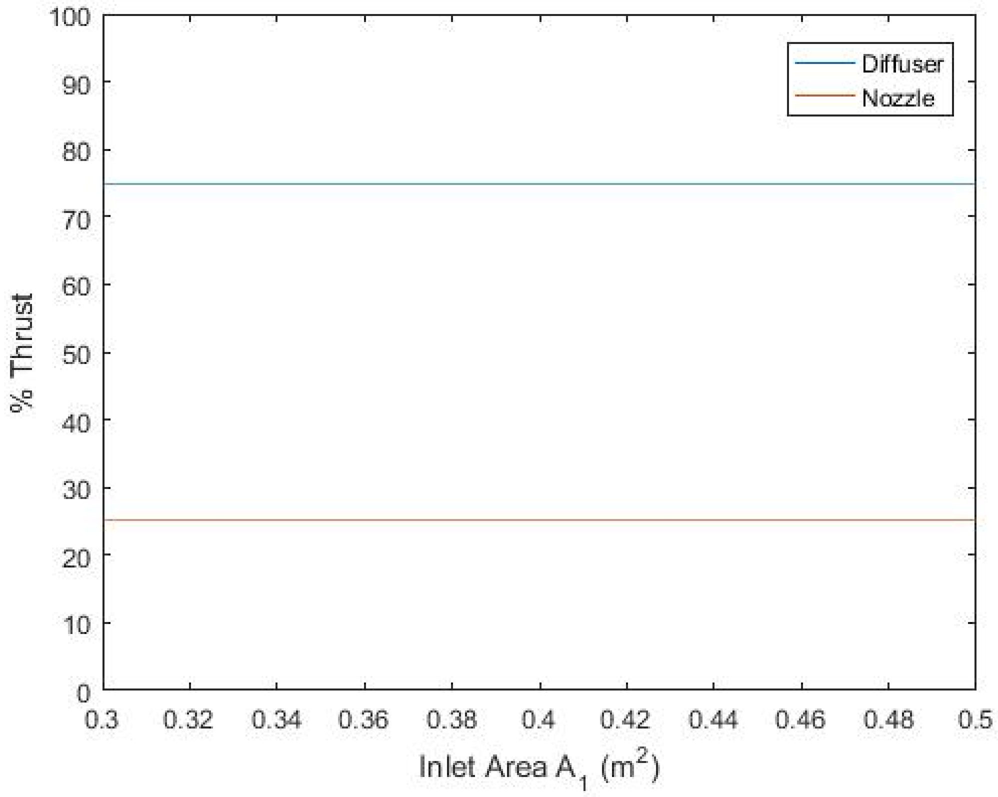

Figure 4.5: Variation of % thrust distribution with A_1 at $M_3 = .23$

Thrust distribution in the diffuser is shown in Fig.4.6. Here D_1 and D_2 represents the converging and diverging part of the diffuser respectively. Converging part of the diffuser produces constant thrust with changing M_3 as the flow there is supersonic and downstream information does not travel upwards. Diverging region thrust decreases with increasing M_3. This happens because inlet conditions to diverging section are constant and does not vary with the change in M_3 while P_3 decreases as combustion inlet Mach number increases (due to expansion), decreasing pressure thrust.

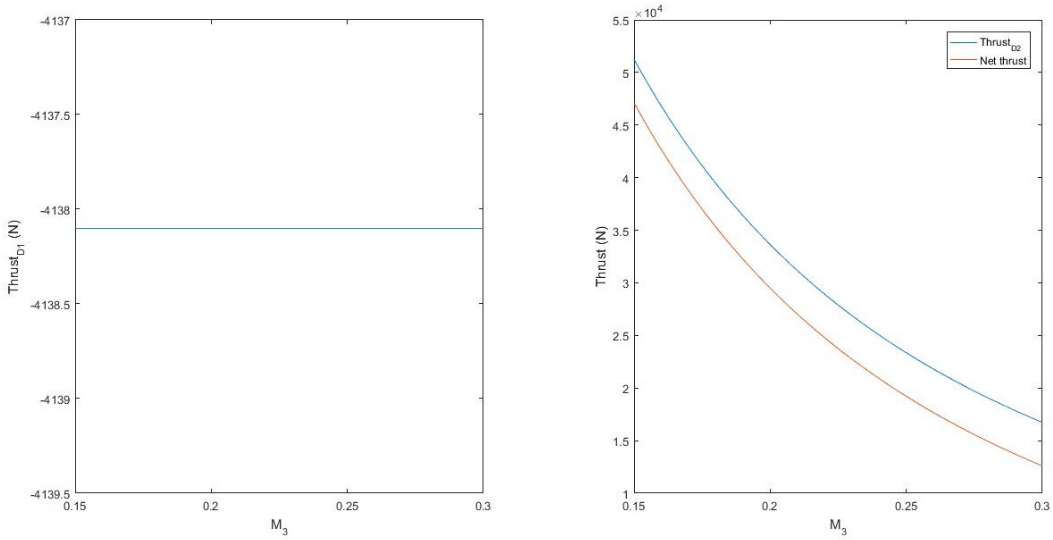

Figure 4.6: Diffuser Thrust with M_3 at $A_1 = 0.3\ m^2$

Nozzle thrust variation with combustion inlet Mach number, M_3 is shown in Fig.4.7. Here N_1 and N_2 represents the converging and diverging part of the nozzle respectively. Thrust depends on the inlet thermodynamic parameters Mach number, pressure and temperature. For converging part, when M_4 increases, T_4 and P_4 are constant and so the thrust here increases but once M_4 becomes constant so does the thrust produced as the pressure forces on the inlet and exit of the converging part almost cancels out each other (taking converging part of the nozzle as control volume).

For the diverging part of the nozzle, inlet Mach number is always one. When T_4 is constant both the Δv, $(v_6 - v_5)$ and P_5 are constant which results in constant thrust production. With decreasing T_4, Δv decreases and so does the thrust. As shown in bottom right figure of Fig.4.7 net thrust produced by nozzle is negative below certain value of combustion inlet Mach number, M_3, which depends on the ramjet inlet Mach number.

Fig.4.8 shows the thrust distribution in the ramjet engine modeled. Fig.4.9 shows the percentage thrust distribution of thrust in all the C-D components.

From the above analysis it is clear that percentage thrust produced by the dif-

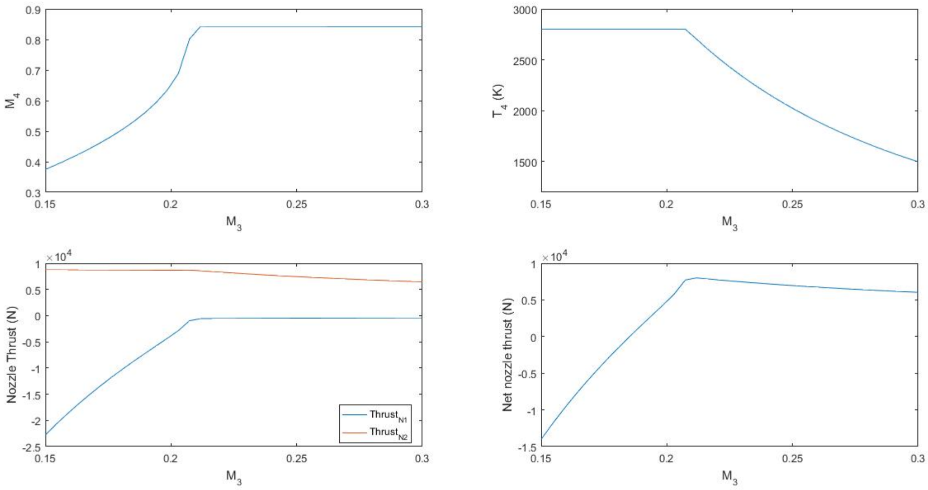

Figure 4.7: Nozzle Thrust with M_3 at $A_1 = .3\ m^2$

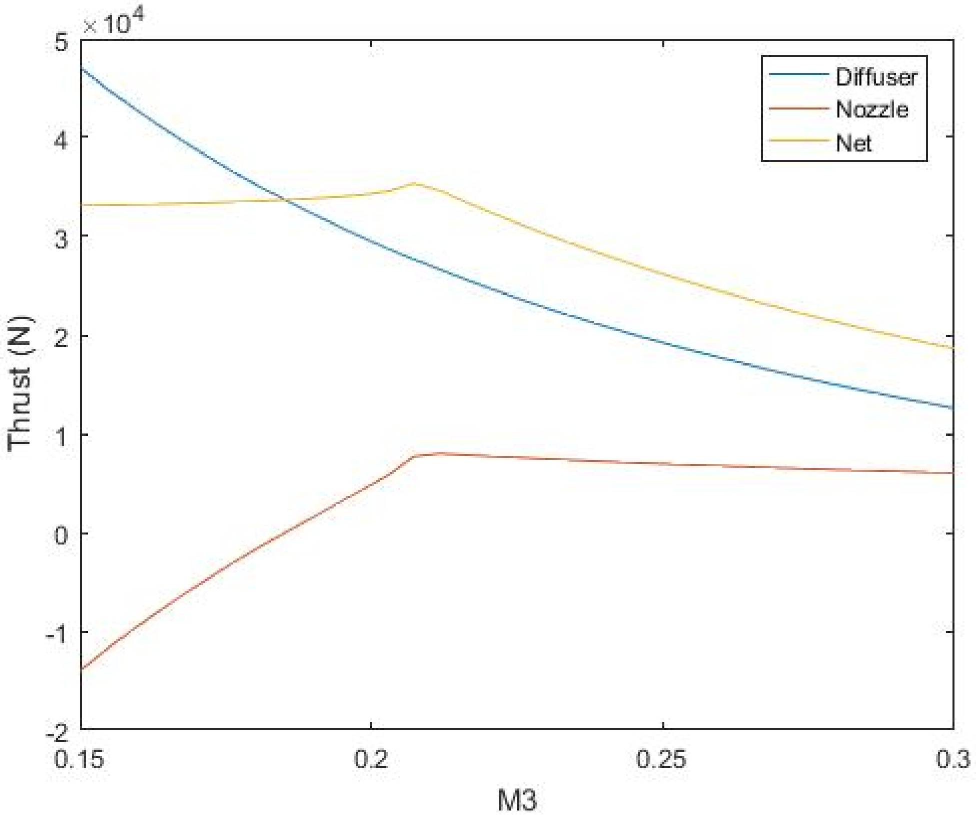

Figure 4.8: Thrust in ramjet with M_3 at $A_1 = .3\ m^2$

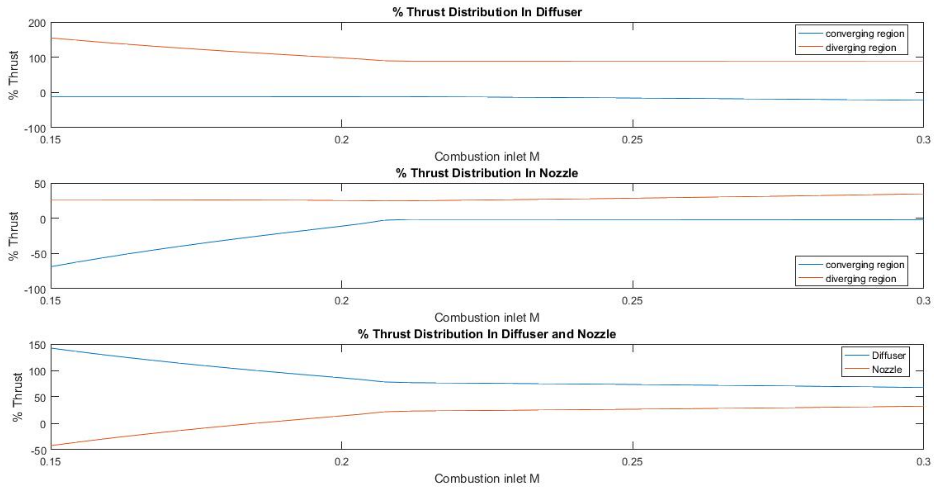

Figure 4.9: % Thrust in ramjet with M_3 at A_1 =.3 m^2

fuser and nozzle is constant with the size of the engine (inlet area) but depends strongly on the combustion inlet temperature, M_3.

Variation of thrust produced by diffuser and nozzle and net thrust is shown in Fig.4.10, Fig.4.11 and Fig.4.12. Net thrust increases with the decrease in combustion inlet Mach number, reaches a maximum and then decreases on further decreasing the combustion inlet Mach number. This happens because diffuser thrust always increases with decrease in M_3 but nozzle thrust produces higher magnitude of negative thrust at low values of M_3. Whereas, thrust increases linearly with increase in the size of the engine (A_1).

As inlet Mach number to the ramjet is increased, M_3 value where T_4 starts to decrease, increases as shown in Fig.4.15. Effect of inlet Mach number on thrust and exit area variation with M_3 is shown in Fig.4.13 and Fig.4.14 respectively.

For the net thrust to be positive, as proved in section *3.4* throat area of nozzle should be greater than throat area of diffuser, which is true here.

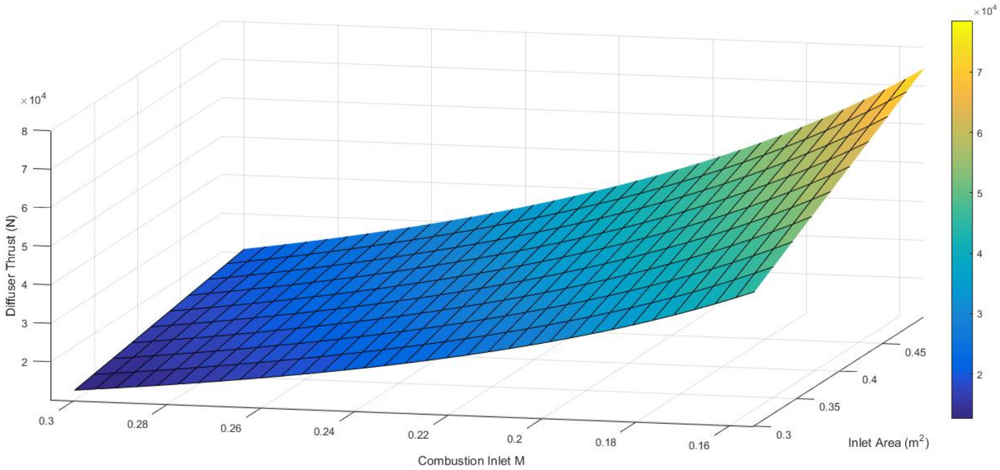

Figure 4.10: Diffuser thrust variation with M_3 and A_1

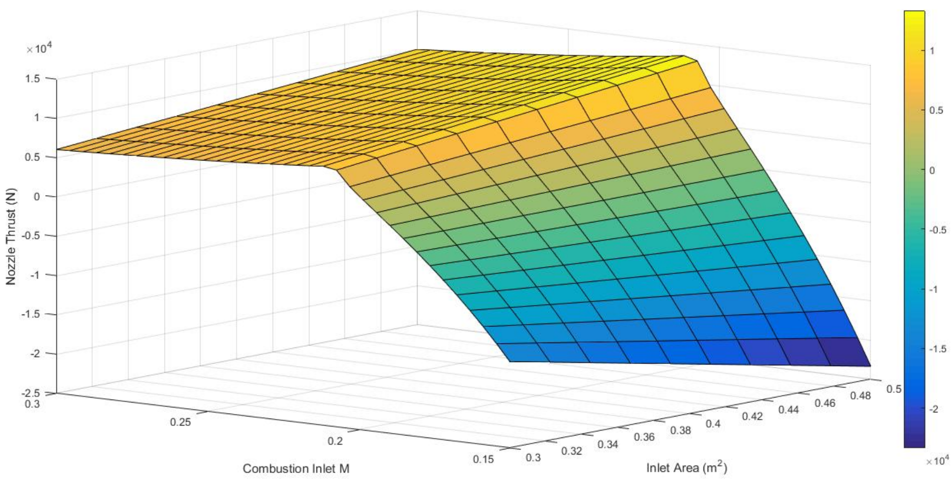

Figure 4.11: Nozzle thrust variation with M_3 and A_1

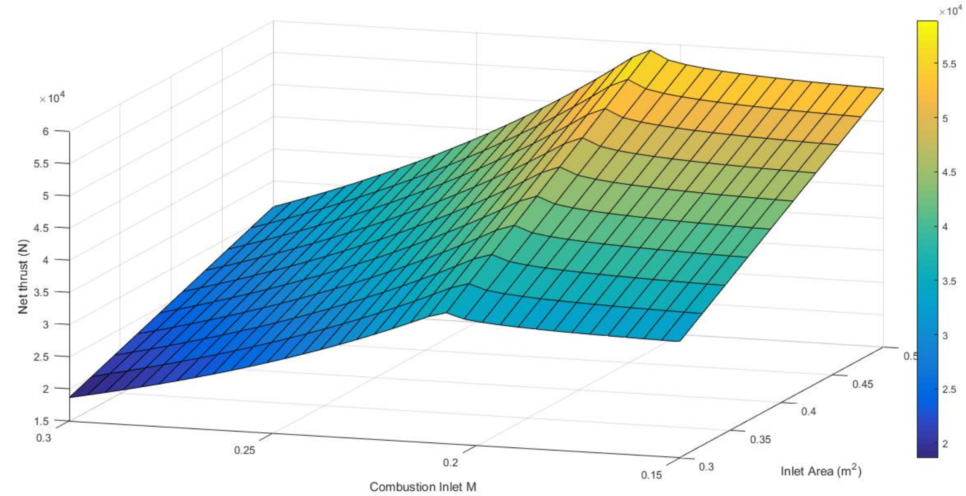

Figure 4.12: Net thrust variation with M_3 and A_1

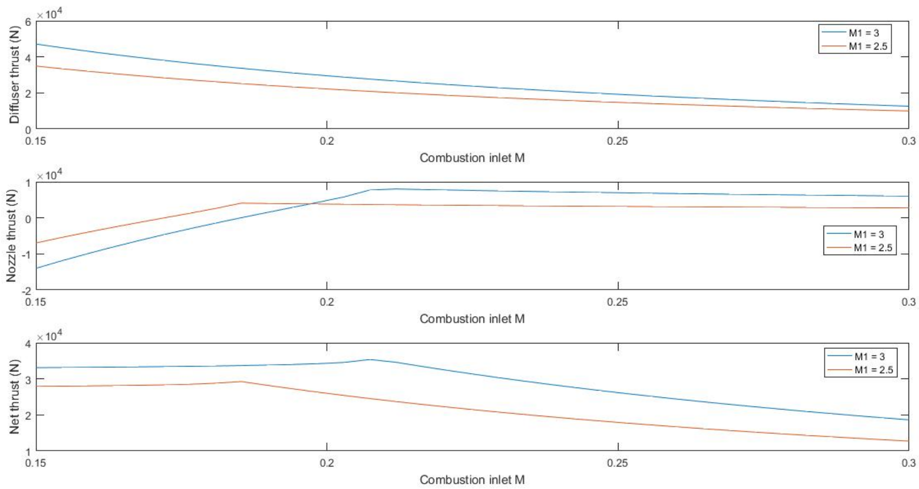

Figure 4.13: Thrust variation with M_3

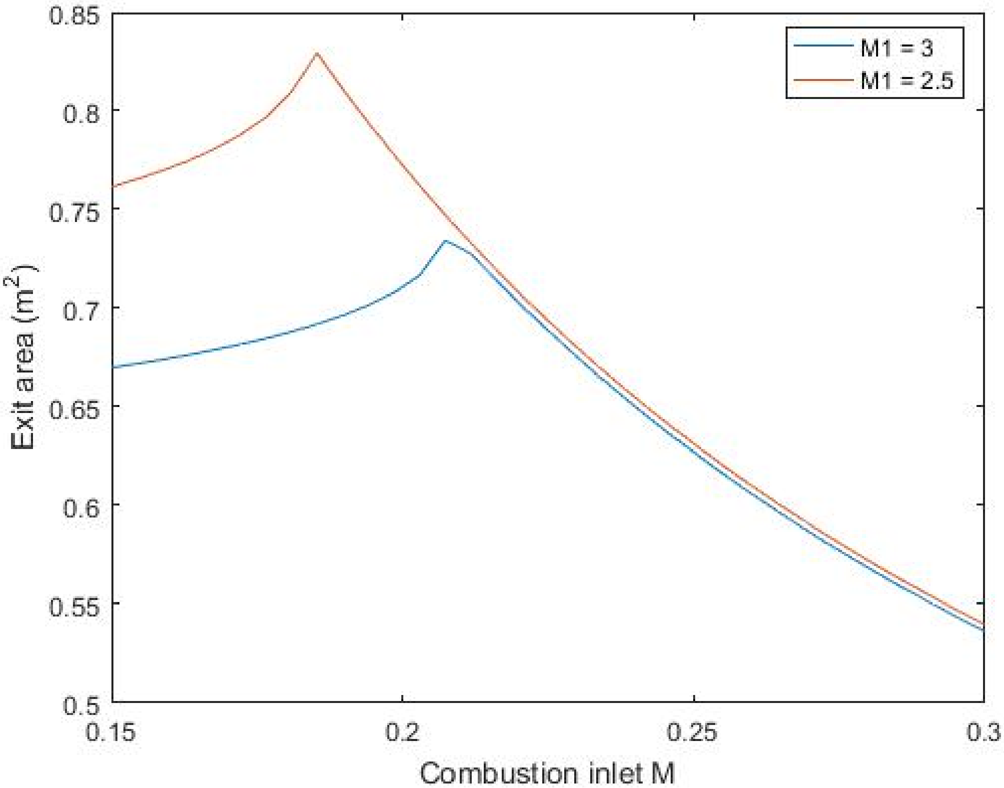

Figure 4.14: Exit area A_6 variation with M_3

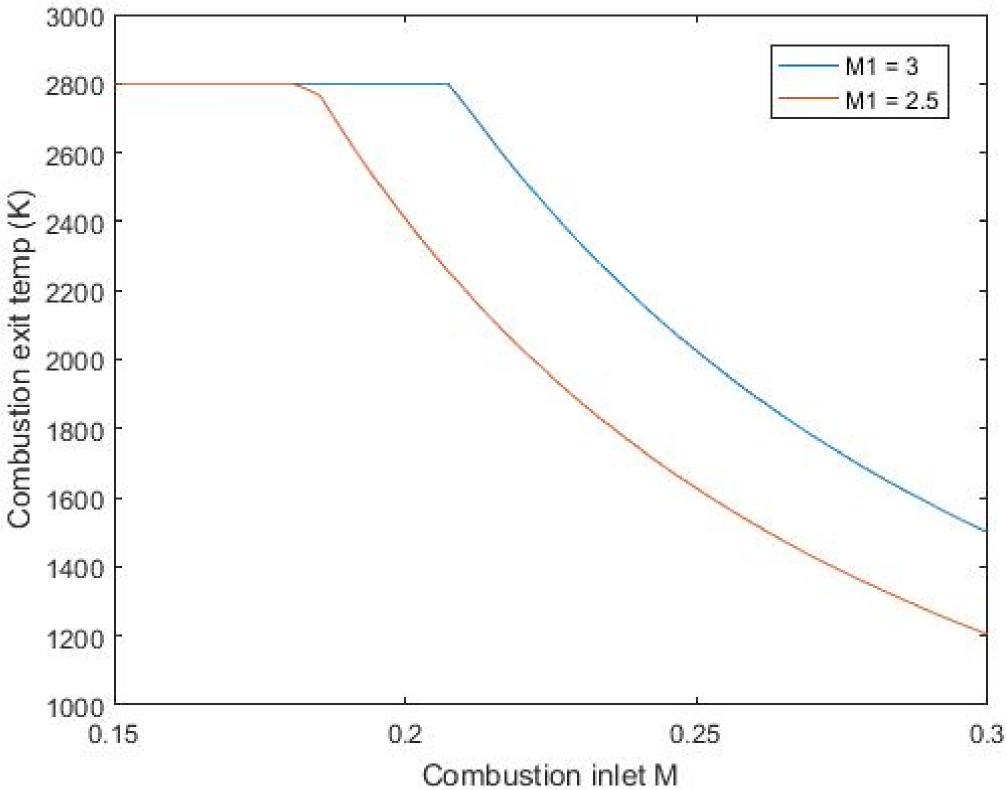

Figure 4.15: Combustion exit temperature T_4 variation with M_3

Chapter 5

Conclusion

In this project I have developed a physical model from first principles to formulate jet propulsion concepts and performance parameters, with the engine as center of interest and not the fluid exchanged as in the conventional approach. The engine thrust is re-defined as the surface integral of pressure forces exerted by the fluid on the surface of the jet engine. Similarly the propulsive efficiency is re-defined as the efficiency with which the pressure forces are utilized for the generation of forward thrust. Two different models of heat addition are analyzed in detail for turbojet engine model. Variable pressure combustor model is then applied to analyze the performance parameters of an ideal ramjet engine.

Chapter 6

Bibliography

[1] [1] Anderson J.D Modern Compressible Flow: With Historical Perspective McGraw-Hill Education; 3 edition (1 August 2002)

[2] [2] Loftin, LK, Jr. "Quest for performance: The evolution of modern aircraft. NASA SP-468". Retrieved 2006-04-22.

[3] [3] Loftin, LK, Jr. "Quest for performance: The evolution of modern aircraft. NASA SP-468 Appendix E". Retrieved 2006-04-22.

[4] [4] Pearson, H., Mixing of Exhaust and Bypass Flow in a Bypass Engine, Journal of the Royal Aeronautical Society, Vol.66, PP 528-530, Aug.62

[5] [5] Philip G. Hill and Carl R. Peterson, Mechanics and Thermodynamics of Propulsion; Addison-Wesley Publishing company

[6] [6] Patrick H. Oosthuizen and William Carscallen, Compressible Fluid Flow 1st Edition ,McGraw-Hill companies, Inc(1997)

[7] [7] Saeed Farokhi, Wiley, Aircraft Propulsion, Second edition.

[8] [8] Wilkinson, Paul H. Aircraft Engines of the world 1946. London: Sir Isaac Pitman & Sons. pp. 298.(2009)

[9] [9] Generation of 1D and 2D grids. In: Numerical Models for Differential Problems. MS&A, vol 2. Springer, Milano